

Synthesis of Walking Primitive Databases for Biped Robots in 3D-Environments

J. Denk and G. Schmidt
Institute of Automatic Control Engineering,
Technische Universität München,
D-80290 Munich, Germany
Joachim.Denk@ei.tum.de, Guenther.Schmidt@ei.tum.de

Abstract—This paper presents a systematic approach to generate walking primitive databases for anthropomorphic 3D-bipeds allowing step length adaptation, direction changes and stepping over obstacles. The individual walking primitives are derived by optimal control techniques. Zero moment point (ZMP) and friction conditions at the feet ensuring postural stability of the biped, as well as bounds on the joint angles and on the control torques, are treated as constraints. The resulting reference trajectories are validated by dynamic simulations.

I. INTRODUCTION

Over the last years, major progress has been made in construction and stabilization of biped walking machines. Gait generation for perception based goal-oriented walking, however, still remains a challenging field of research [1]. Locomotion in a partly unknown environment requires the ability of a biped to adapt its gait pattern according to the present situation, so that obstacles in the walking trail can be passed by or overcome. But, unlike industrial robots, bipeds are not fixed rigidly to the ground and have the tendency to tip over very easily. Their postural stability depends on the behaviour of six unpowered degrees of freedom (DoF) defining their pose in the world, which can only be influenced indirectly by appropriate actuation of the powered DoF in the joints. The control problem of executing stable steps is therefore usually based on an adequate reference trajectory, i.e. a walking pattern. As a consequence of the high nonlinearity and complexity of the system, however, it is not possible in general to compute a walking pattern online, while taking all dynamical properties of a 3D biped into account. Hence, methods for online walking pattern generation are usually based on simplified robot models and rely on feedback control [2]. One possible approach for gaining more accurate reference trajectories online is to split the problem in two parts. First, a series of walking primitives (WPs) for steps with different step parameters, like step length or step clearance, is computed offline and stored in a database. Using information about obstacles in the walking trail provided by a perception system, a step sequence planner can then select and concatenate appropriate WPs during runtime in order to obtain a situation dependent walking pattern [3–6].

This paper deals with a systematic approach, which is suited for synthesizing databases of dynamically or statically stable WPs [7] automatically and in feasible time using optimal control techniques [8–10]. The WPs in the database are synthesized such that they can be concatenated in a reference trajectory allowing step length adaptation, changes in direction and stepping over obstacles. As a validation of the reference trajectories, results of dynamic simulations are presented.

In Section II the problem of WP database generation is formulated and the class of biped walking machines considered is defined. The

search space for the proposed general WPs is characterized in Section III. After a discussion of the dynamic modeling approach used in Section IV, the optimal control problem is summarized in Section V. Numerical results gained by applying the method to the model of an anthropomorphic 3D-biped with 12 joints are presented in Section VI. After general considerations about the derivation of symmetric steps and about WP concatenation, the necessary procedure for WP database generation is discussed in Section VIII. It is shown, how cyclic, transition, curve and barrier WPs can be gained by specialization of general WPs. Section IX presents results of a dynamic simulation of a step sequence comprising step length adaptation, direction changes and stepping over obstacles.

II. PROBLEM FORMULATION

We consider walking machines of the type illustrated in Fig. 1 consisting of bodies B_i , $i = 1 \dots N_b$, connected by driven joints with the joint angles q_i and control torques τ_i , $i = 1 \dots N_j$, respectively. Symmetry of the biped's left and right side is assumed to allow a symmetric gait. The legs have to comprise at least six powered joints each, allowing to manipulate the feet in 6 DoF in Cartesian space relative to the torso. Further joints in the biped's torso are not considered in this work, but could be regarded in principle.

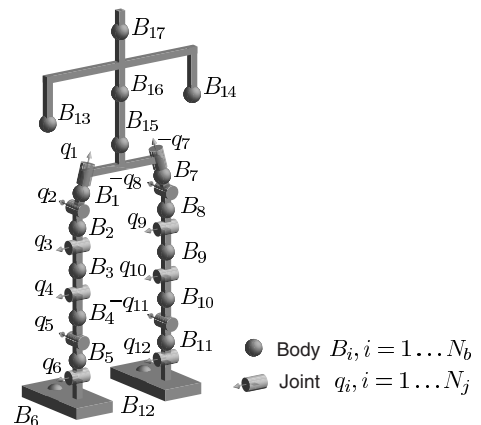


Fig. 1. Kinematic scheme of biped robot with $N_b = 17$ bodies B_i and $N_j = 12$ driven joints.

As input to the problem, the biped's kinematical parameters, all necessary dimensions, the masses and inertia tensors of the bodies B_i , the restrictions on joint angles q_i and joint velocities \dot{q}_i , the maximum allowed motor torques and the coefficients of friction between the feet and the ground have to be provided.

The joint angles $\mathbf{q}_l = [q_1 \dots q_{N_j/2}]^T$ of the left leg and $\mathbf{q}_r = [q_{N_j/2+1} \dots q_{N_j}]^T$ of the right leg are then subsumed in the vector

$\mathbf{q} = [\mathbf{q}_l, \mathbf{q}_r]$. Accordingly, joint torques are subsumed in $\boldsymbol{\tau} = [\boldsymbol{\tau}_l, \boldsymbol{\tau}_r]$. Four coordinate systems are defined, namely the world coordinate system S_O and the contact frames S_L and S_R fixed in the sole of the left and right foot respectively. The contact coordinate system S_A is needed to describe the contact situation of the right foot, if the foot is rotated with respect to the left foot, see Fig. 2. The pose of S_L , S_R and S_A with respect to S_O is given by $\mathbf{p}_L = [\mathbf{r}_L, \boldsymbol{\phi}_L]$, $\mathbf{p}_R = [\mathbf{r}_R, \boldsymbol{\phi}_R]$ and $\mathbf{p}_A = [\mathbf{r}_A, \boldsymbol{\phi}_A]$. The components of vector $\mathbf{r} = [r_x \ r_y \ r_z]^T$ are Cartesian coordinates. $\boldsymbol{\phi} = [\phi_x \ \phi_y \ \phi_z]^T$ are orientations represented by roll-, pitch-, and yaw-angles. The posture of the biped is defined by the generalized coordinates $\mathbf{q}_{g,R} = [\mathbf{q}, \mathbf{p}_L]$ during a step with the right and $\mathbf{q}_{g,L} = [\mathbf{q}, \mathbf{p}_R]$ during a step with the left leg.

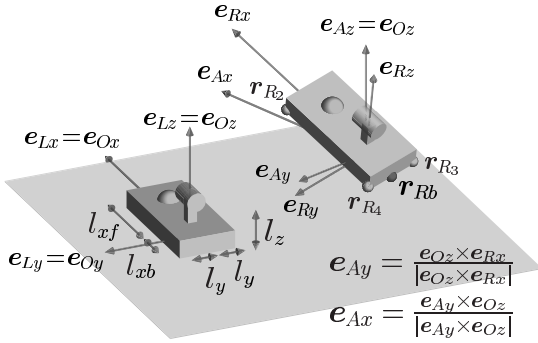


Fig. 2. Biped feet with world coordinate system S_O , left/right foot frame S_L/S_R , contact frame S_A , lengths l , and points \mathbf{r} . The left foot frame S_L coincides with S_O , the derivation of S_A is given.

To provide the described biped with the reference trajectories needed for locomotion in 3D-scenarios, a database of WPs allowing straight ahead walking with step length adaptation, changing direction and striding over obstacles has to be synthesized. The individual primitives $\Upsilon(t) = [\mathbf{q}(t), \boldsymbol{\tau}(t)]$, $t \in [0, t_s]$ need to be computed in such a way, that they can be concatenated in real time resulting in the control torques $\boldsymbol{\tau}_{ref}(t)$ required for driving the biped along a smooth and physically feasible joint trajectory $\mathbf{q}_{ref}(t)$ while maintaining a defined behaviour $\mathbf{p}_{L,ref}(t)$ resp. $\mathbf{p}_{R,ref}(t)$ of the unpowered DoF.

III. SEARCH SPACE SPECIFICATION FOR A GENERAL WP

In the following subsections, the search space of the optimal control problem for a single general walking primitive is defined. A general walking primitive corresponds to a single step with the right foot swinging. Due to the assumed symmetry of the biped robot, however, a symmetric step for the left foot swinging can be derived by a simple mapping, which will be explained in Section VII-A.

A. Kinematics of Walking Primitive

The considered WPs comprise the 3 phases *pre-swing*, *swing* and *heel-contact*, see Fig. 3 and Fig. 4. The left foot resides flat on the ground during the whole motion, given by $\mathbf{p}_L(t) = [r_x^0 \ r_y^0 \ r_z^0 \ 0 \ 0 \ \phi_z^0]^T$, $\forall t \in [0, t_s]$. Using the transformation $\mathbf{q}_{g,R}(t) = [\mathbf{q}(t), \mathbf{p}_L(t)]$, $\forall t \in [0, t_s]$ the system can be described in minimal coordinates $\mathbf{q}(t)$ for this contact situation reducing the number of system states during walking primitive synthesis from $2 \times (N_j + 6)$ to $2 \times N_j$. Thus, the system state is given by $\mathbf{x}(t) = [\mathbf{q}(t), \dot{\mathbf{q}}(t)]$ in the follow-

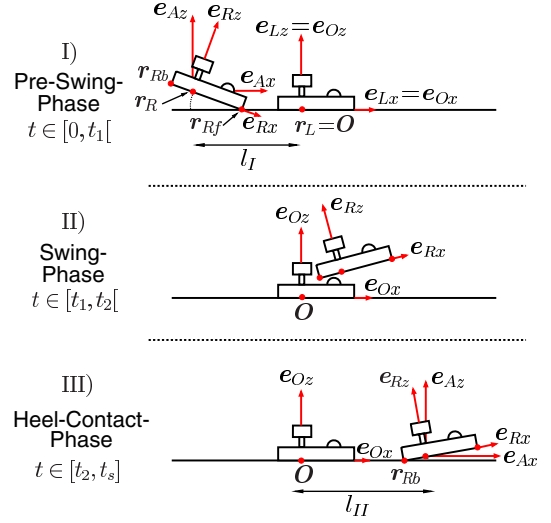


Fig. 3. Three phases of WP, side view.

ing. However, it is obvious, that the feasibility of a walking primitive will not depend on the parameters $r_x^0, r_y^0, r_z^0, \phi_z^0$ since they do not influence the attitude of the biped with respect to the gravity vector ${}^O\mathbf{g} = [0 \ 0 \ -1]^T$. Therefore, in order to simplify the discussion and without loss of generality, the left foot of the biped is assumed to be positioned in the origin of the world coordinate system according to $\mathbf{p}_L(t) = \mathbf{0}$ during WP synthesis, see Fig. 2. During *swing-phase II*, the mechanism of the biped forms an open kinematic chain. During *pre-swing I* and *heel-contact III*, however, both feet contact the ground thus forming a closed chain. This hybrid character is taken into account by kinematic constraints imposed on the system accelerations. Step length of the previous step l_I , step length l_{II} , step widths w_0, w_s , angles ϕ_0, ϕ_s corresponding to a rotation of the right foot with respect to the left foot in *pre-swing I* resp. *heel-contact III*, as well as phase-transition-times t_1, t_2 and step-duration t_s are used to parameterize the motion.

In order to avoid undesirable mechanical stress, the trajectory $\mathbf{q}(t)$ is constrained to be smooth, i.e. continuous and continuously differentiable with respect to time. This implies that there are no jumps in the Cartesian velocities of the right foot and thus impacts are avoided when the heel contacts the ground.

I) Pre-Swing-Phase ($t \in [0, t_1[$):

The WP starts with the right foot located flat on the ground at $t = 0$. Pose and velocity are given by

$$\mathbf{p}_R(0) = \begin{bmatrix} -l_I & -w_0 & 0 & 0 & 0 & \phi_0 \end{bmatrix}^T \quad (1)$$

$$[{}^A\dot{\mathbf{r}}_R(0), {}^A\boldsymbol{\omega}_R(0)] = \mathbf{C}_R(\mathbf{q}(0)) \dot{\mathbf{q}}(0) = \mathbf{0},$$

where $\mathbf{C}_R \in \mathbb{R}^{6 \times N_j}$ is a Jacobian matrix mapping the joint velocities $\dot{\mathbf{q}}(t)$ to the Cartesian velocities ${}^A\dot{\mathbf{r}}_R$ and angular velocities ${}^A\boldsymbol{\omega}_R$ of the right foot represented in the contact frame A . The respective initial system state is denoted $\mathbf{x}_0 = [\mathbf{q}_0, \dot{\mathbf{q}}_0] = [\mathbf{q}(0), \dot{\mathbf{q}}(0)]$. During $t \in [0, t_1[$, the right foot rolls over the toes. This contact situation is expressed by the kinematic constraint

$$[{}^A\ddot{\mathbf{r}}_{Rf}(t), {}^A\dot{\omega}_{R,x}(t), {}^A\dot{\omega}_{R,z}(t)] = \frac{d}{dt} [\mathbf{C}_{Rf}(\mathbf{q})\dot{\mathbf{q}}] = \mathbf{0}, \quad (2)$$

where \mathbf{r}_{Rf} is a point at the toes of the foot and $\mathbf{C}_{Rf} \in \mathbb{R}^{5 \times N_j}$ a

Jacobian, see Fig. 4. The heel stays above ground which is ensured by the inequality constraint $r_{Rb,z}(t) \geq 0$.

II) Swing-Phase ($t \in [t_1, t_2[$):

The *swing-phase II* starts with the right foot just about to leave the ground at $t = t_1$ and then swinging towards its new position. Inequality constraints are used to avoid collisions with the ground or the left leg.

III) Heel-Contact-Phase ($t \in [t_2, t_s]$):

At $t = t_2$, the foot touches the ground and rolls around the heel during $t \in [t_2, t_s[$. The corresponding kinematic constraint is given by

$$[A\ddot{\mathbf{r}}_{Rb}(t), A\dot{\omega}_{R,x}(t), A\dot{\omega}_{R,z}(t)] = \frac{d}{dt} [\mathbf{C}_{Rb}(\mathbf{q})\dot{\mathbf{q}}] = \mathbf{0} \quad (3)$$

where \mathbf{r}_{Rb} is a point at the heel of the foot and $\mathbf{C}_{Rb} \in \mathbb{R}^{5 \times N_j}$ a Jacobian, see Fig. 4. The toes need to remain above ground, which is ensured by $r_{Rf,z}(t) \geq 0$. The WP ends at $t = t_s$, when the right foot is flat on the ground again. Pose and velocity are given by

$$\begin{aligned} \mathbf{p}_R(t_s) &= [l_{II} \quad -w_s \quad 0 \mid 0 \quad 0 \quad \phi_s]^T \\ [A\dot{\mathbf{r}}_R(t_s), A\dot{\omega}_R(t_s)] &= \mathbf{C}_R(\mathbf{q}(t_s)) \dot{\mathbf{q}}(t_s) = \mathbf{0}. \end{aligned} \quad (4)$$

The final system state is denoted $\mathbf{x}_s = [\mathbf{q}_s, \dot{\mathbf{q}}_s] = [\mathbf{q}(t_s), \dot{\mathbf{q}}(t_s)]$.

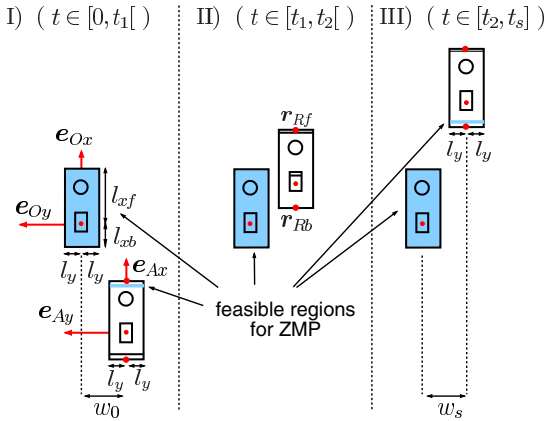


Fig. 4. Three phases of WP and feasible regions for ZMP, top view. ($\phi_0 = \phi_s = 0$, i.e. no rotation of right foot with respect to left foot.)

B. Conditions for Contact Stability

In all forms of walking, physical contacts between a foot and the ground are unilateral. Stability of the contact situation during the three walking phases defined in Section III-A thus requires the occurring contact forces to conform with the contact stability conditions summarized next. The sum of all forces on a contact surface is thereby represented by the resultant contact forces $\mathbf{f} = [f_x \quad f_y \quad f_z]^T$ and moments $\mathbf{n} = [n_x \quad n_y \quad n_z]^T$ acting in the points $\mathbf{r}_L, \mathbf{r}_{Rf}, \mathbf{r}_{Rb}$ depending on the current walking phase, see Fig. 5.

• **Unilaterality Conditions** on the resultant normal contact forces ensure, that a desired contact situation does not change by a foot lifting off the ground, i.e. $Lf_{L,z} \geq 0$ during all three phases for the left foot and $Af_{Rf,z} \geq 0$ during *pre-swing I* resp. $Af_{Rb,z} \geq 0$ during *heel-contact III* for the right foot.

• **ZMP Conditions** [11] are used in this work to prevent a foot from beginning to rotate around its edges. The ZMP $\mathbf{r}_p = [r_{p,x} \quad r_{p,y} \quad 0]^T$ is defined as the point on the contact surface, where the resultant moments n_x, n_y of all contact forces are zero. The contact situation is

stable, if the ZMP remains inside the contact area. The ZMP \mathbf{r}_{pL} of the left foot can be expressed in the left foot frame L as

$$Lr_{pL,x} = -\frac{Ln_{L,y}}{Lf_{L,z}}, \quad Lr_{pL,y} = \frac{Ln_{L,x}}{Lf_{L,z}}.$$

Inequality constraints prevent the ZMP from leaving the area of valid ZMP positions illustrated in Fig. 4 and ensure that the foot remains flat on the ground during all three phases. As the right foot rotates around its front edge during *pre-swing I* there is no resultant moment $An_{Rf,y}$ and the contact surface degenerates to a line. The ZMP of the right foot moves along this line while its coordinates in frame S_R are given by

$$Rr_{pR,y} = \frac{An_{Rf,x}}{Af_{Rf,z}}, \quad Rr_{pR,x} = l_{xf} \quad (5)$$

By preventing Rr_{pR} from leaving the left or right edge of the foot, see Fig. 4, rotations around the x-axis e_{Ax} are avoided. The situation during *heel-contact III* is treated accordingly.

• **Friction Conditions** must ensure that a supporting foot neither begins to slip on the ground nor starts to rotate around the normal axis e_z of the contact surface. Thus the friction condition [7]

$$\sqrt{f_x^2 + f_y^2} + \left| \frac{n_z}{\kappa} \right| \leq \mu f_z \quad (6)$$

is applied. The constant $0 < \mu < 1$ denotes the friction coefficient of the rubbing surfaces and κ is the frictional radius. The assumed frictional radius for the left foot is $\kappa_L = 0.5\sqrt{(2l_y)^2 + (l_{xb} + l_{xf})^2}$ and for the right foot $\kappa_{Rf} = \kappa_{Rb} = l_y$ during both *pre-swing* phase and *heel-contact* phase.

C. Mechanical and Electrical Restrictions

Physical admissibility of the WPs also demands compliance with restrictions given by the performance limits of the motors and by the mechanical mechanism. This is regarded by inequality constraints defining maximum and minimum values for the joint angles $\mathbf{q}(t)$, joint velocities $\dot{\mathbf{q}}(t)$, and joint torques $\boldsymbol{\tau}(t)$.

IV. DYNAMIC MODELING

The system dynamics in the three phases of a WP are modeled under the assumption of bilateral rigid body contacts between the feet and the ground. Since the conditions for contact stability formulated in Section III-B prevent the occurrence of contact forces which are not compatible with the actual unilateral contact situation, this modeling is permissible. The dynamics of the biped in minimal coordinates $\mathbf{q}(t) \in \mathbb{R}^{N_j}$ are then given by

$$\mathbf{M}\ddot{\mathbf{q}} = \mathbf{h} + \boldsymbol{\tau} + \mathbf{C}_{Rf}^T A\mathbf{F}_{Rf} + \mathbf{C}_{Rb}^T A\mathbf{F}_{Rb} \quad (7)$$

with the mass-matrix $\mathbf{M}(\mathbf{q})$, coriolis, centrifugal, and gravity effects $\mathbf{h}(\mathbf{q}, \dot{\mathbf{q}})$, and joint torques $\boldsymbol{\tau}$. The Jacobians $\mathbf{C}_{Rf}(\mathbf{q}) \in \mathbb{R}^{5 \times N_j}$ and $\mathbf{C}_{Rb}(\mathbf{q}) \in \mathbb{R}^{5 \times N_j}$ from Eq. (2) and Eq. (3) are projecting the generalized constraint contact forces $A\mathbf{F}_{Rf} = [Af_{Rf}, An_{Rf,x}, An_{Rf,z}] \in \mathbb{R}^{5 \times 1}$ and $A\mathbf{F}_{Rb} = [Af_{Rb}, An_{Rb,x}, An_{Rb,z}] \in \mathbb{R}^{5 \times 1}$ on the generalized coordinates. Since the contact situation of the left foot is formulated in minimal coordinates, the forces $L\mathbf{F}_L = [Lf_L, Ln_L] \in \mathbb{R}^{6 \times 1}$ are not part of the dynamic system equations. However, they can be recalculated easily using the Principle of D'Alambert as soon as $\ddot{\mathbf{q}}$ and the external forces on the right foot have been determined, see also [7].

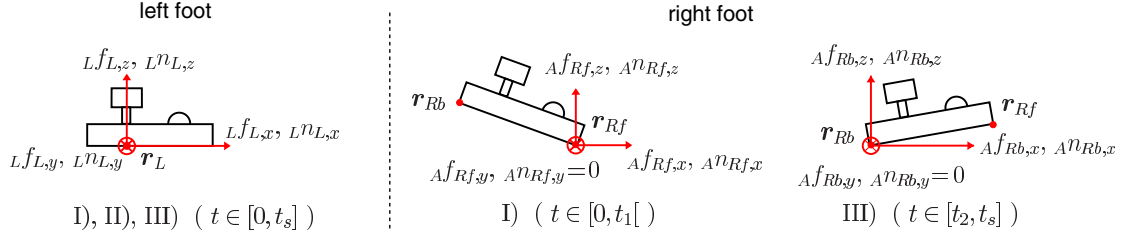


Fig. 5. Contact forces at left and right foot during phases of WP.

The system accelerations during *swing-phase II* (${}^A\mathbf{F}_{Rb} = {}^A\mathbf{F}_{Rf} = \mathbf{0}$) are computed as

$$\ddot{\mathbf{q}} = \mathbf{M}^{-1}(\mathbf{h} + \boldsymbol{\tau}). \quad (8)$$

During *pre-swing I* (${}^A\mathbf{F}_{Rb} = \mathbf{0}$) resp. *heel-contact III* (${}^A\mathbf{F}_{Rf} = \mathbf{0}$) the 5 additional equations Eq. (2) resp. Eq. (3) on the system accelerations can be used together with Eq. (7) to solve for $[\ddot{\mathbf{q}}, {}^A\mathbf{F}_{Rf}]$ resp. $[\ddot{\mathbf{q}}, {}^A\mathbf{F}_{Rb}]$ resulting in:

$$\begin{aligned} \ddot{\mathbf{q}} &= \mathbf{M}^{-1}(\mathbf{h} + \boldsymbol{\tau} + \mathbf{C}_{Rf/b}^T {}^A\mathbf{F}_{Rf/b}) \\ {}^A\mathbf{F}_{Rf/b} &= -(\mathbf{C}_{Rf/b} \mathbf{M}^{-1} \mathbf{C}_{Rf/b}^T)^{-1} \\ &\quad (\mathbf{C}_{Rf/b} \mathbf{M}^{-1}(\mathbf{h} + \boldsymbol{\tau}) + \dot{\mathbf{C}}_{Rf/b} \dot{\mathbf{q}}) \end{aligned} \quad (9)$$

V. OPTIMAL CONTROL PROBLEM

The search space for a WP defined in Section III together with the system dynamics derived in Section IV specify a whole family of feasible motions. By solving an optimal control problem the WP is selected, which minimizes a mixed performance index. The applied performance index is based on the mechanical power $P_i(t) = \dot{q}_i(t)\tau_i(t)$ transmitted by a motor in the i -th joint, c.f. [9, 10, 12]:

$$\begin{aligned} \min_{\boldsymbol{\tau}(t)} &\left(\int_0^{t_1} \sum_{i=1}^{N_j} \left| \frac{P_i(t)}{P_n} \right| dt + \int_{t_1}^{t_2} \left(\sum_{i=1}^{N_j} \left| \frac{P_i(t)}{P_n} \right| + \right. \right. \\ &\quad \left. \left. + \sum_{j=1}^4 e^{\alpha(\epsilon - r_{R_j,z})} \right) dt + \int_{t_2}^{t_s} \sum_{i=1}^{N_j} \left| \frac{P_i(t)}{P_n} \right| dt \right) \end{aligned}$$

with t_1, t_2 and t_s given and fixed; P_n , α and ϵ are constant parameters. The additional term during *swing-phase II* depends on the position of the contact points \mathbf{r}_{R_j} , $j = 1 \dots 4$, see Fig. 2, and penalizes the right foot being too close to the ground.

This functional needs to be minimized subject to the differential equations of the system according to the actual motion phase, the contact stability conditions and the inequality constraints for collision avoidance. Phase connection conditions on the system state at $t = t_1$ and $t = t_2$ must ensure a continuous state trajectory. Furthermore, the inequality constraints on the joint angles, joint velocities and joint torques are needed to regard restrictions given by the mechanical and electrical design. To allow WP concatenation, additional boundary conditions on the initial state \mathbf{x}_0 and final state \mathbf{x}_s are required. These boundary conditions depend on the special type of the walking primitive. They are going to be discussed in Section VIII.

VI. OPTIMIZATION RESULTS FOR A CYCLIC WP

The described method was applied to the model of the biped robot ‘‘Johnnie’’ developed at TU Munchen [13]. Its kinematics is illustrated

in Fig. 1. Three joints are located in each hip, one joint in the knees and two joints in the ankles. For simplification, additional joints located in the upper body of Johnnie are not regarded during the optimization process.

The optimal control problems are solved using the direct-collocation software DIRCOL [14]. DIRCOL converts the continuous optimal control problem into a static optimization problem by discretization of trajectories in time and by representing the system states $\mathbf{x}(t)$ by cubic spline and the controls $\boldsymbol{\tau}(t)$ by piecewise linear functions. Compliance with the differential equations of the system is ensured by the spline parameterization and equality constraints [14]. The resulting nonlinear programming problem is then solved by the sparse solver SNOPT [15]. All necessary dynamical equations are derived with the help of AUTOLEV [16], a tool for analytical motion analysis.

As an example, optimization results gained for a cyclic WP with step length $l_I = l_{II} = 0.5\text{m}$, step-width $w_0 = w_s = 0.23\text{m}$, rotation of the right foot $\phi_0 = \phi_s = 0^\circ$, step time $t_s = 1.1\text{s}$ and phase transition times $t_1 = 0.09 t_s$ resp. $t_2 = 0.95 t_s$ are presented. A detailed discussion about properties of a cyclic WP follows in Section VIII. The resulting foot motion is depicted in Fig. 6. The paths of the ZMPs of the left and right foot \mathbf{r}_{pL} and \mathbf{r}_{pR} during the three phases as well as the projection of the center of mass (PCOM) to the ground are shown in Fig. 7.

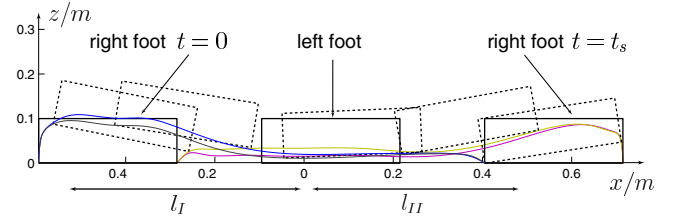


Fig. 6. Path of right foot for cyclic WP with $l = 0.5\text{m}$.

As desired, the ZMP \mathbf{r}_{pL} moves inside the supporting area of the left foot during the whole *swing-phase II* indicating a stable contact situation. It can also be noted, that the PCOM is outside the supporting area during part of the *swing-phase II*. This fact indicates, that the corresponding motion is dynamically stable [7]. Clearly, the PCOM would remain inside the supporting area during the whole *swing-phase II*, too, if the step time t_s was increased. This would indicate statically stable walking.

Details concerning the generation of the initial solutions needed for starting the optimization problems, computational requirements and computational time need can be found in [12]. Typical computation times vary between a few minutes and a few hours depending on the quality of the initial solution. By starting optimization runs for new WPs with previously gained solutions for similar problems in a system-

atic way, convergence can be greatly enhanced. This allows to compute huge numbers of WPs automatically [12].

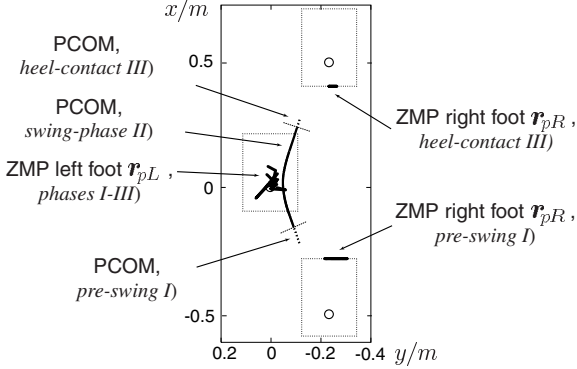


Fig. 7. Path of ZMP and PCOM for cyclic WP, $l=0.5m$.

VII. CONCATENATION OF WPS

As discussed in Section II, WPs for different step lengths, different changes in direction and different obstacles have to be computed such, that they can be concatenated into a smooth reference trajectory. The necessary derivation of symmetric steps and the conditions for WP concatenation are discussed in the following. It is assumed, that a left step is always followed by a right step and vice versa.

A. Derivation of Symmetric Steps: WP Mapping

The demanded symmetry in the biped model allows to directly derive a WP $\tilde{\Upsilon}(t)$ for the left foot swinging while the right foot is supporting the biped from a generated WP $\Upsilon(t)$. This is easily achieved by interchanging the joint angles and joint torques of the left and right leg, since the direction of rotations of the joints is chosen appropriately, see signs of q_i in Fig. 1. Interchanging the joint angles is performed by the mapping

$$\tilde{q}(t) = [q_r(t), q_l(t)], \quad t = [0, t_s]. \quad (10)$$

Respective joint torques $\tau(t)$ are mapped accordingly. A mapped WP is thus given by $\tilde{\Upsilon}(t) = [\tilde{q}(t), \tilde{\tau}(t)]$.

B. Conditions for WP Concatenation

Concatenation of an arbitrary WP $\Upsilon^i(t)$, $t = [0, t_s^i]$ for a right step and an arbitrary WP $\tilde{\Upsilon}^{i+1}(t)$, $t = [0, t_s^{i+1}]$ for a left step is defined as

$$\Upsilon^i(t) | \tilde{\Upsilon}^{i+1}(t) = \begin{cases} \Upsilon^i(t) & , t = [0, t_s^i] \\ \tilde{\Upsilon}^{i+1}(t - t_s^i) & , t = [t_s^i, t_s^i + t_s^{i+1}] \end{cases}.$$

For the physical feasibility of the resulting trajectory, the initial state of $\tilde{\Upsilon}^{i+1}(t)$ and final state of $\Upsilon^i(t)$ must satisfy the conditions for walking primitive concatenation

$$\tilde{x}_0^{i+1} = x_s^i \quad (11)$$

ensuring, that the resulting joint trajectory $q_{ref}(t)$ is smooth. Obviously, if Eq. (11) is satisfied for a right/left combination $\Upsilon^i(t) | \tilde{\Upsilon}^{i+1}(t)$, the left/right combination $\tilde{\Upsilon}^i(t) | \Upsilon^{i+1}(t)$ is physically feasible, too.

VIII. PROCEDURE FOR WP DATABASE GENERATION

To gain a reference trajectory allowing to walk around or step over obstacles in a 3D-environment, a database of WPs has to be generated. This database must comprise cyclic WPs ${}^C\Upsilon^l$ to walk with a constant step length l and transition WPs ${}^T\Upsilon^{l_1 \sim l_2}$ for step length adaptation. Furthermore, combinations of two curve WPs ${}^{D,I}\Upsilon^{l_1 \sim l_2, \phi}$, ${}^{C,II}\Upsilon^{l_2 \sim l_3, \phi}$ to change the walking direction by an angle $\pm\phi$, see Fig. 10, and combinations of two barrier WPs ${}^{B,I}\Upsilon^{l_1 \sim l_2, c}$, ${}^{B,II}\Upsilon^{l_2 \sim l_3, c}$ to execute steps with clearance c allowing to step over obstacles, see Fig. 9, are needed. WPs for stair climbing, starting and stopping can be regarded accordingly, but they are not discussed in the context of this paper. To allow WP concatenation, the database has to be planned and synthesized such that the initial and final states x_0 and x_s of individual WPs fulfill the conditions for WP concatenation, see Eq. (11).

A. Graph representation of WP database

As a first step for WP database generation it must be determined, which WPs are required in the walking task of the robot. Thereby, the scenario, requirements of the algorithm for step sequence planning [6], precision of image processing, a priori known restrictions of the biped, e.g. step length restrictions, and the complexity of the database [12, 17] must be taken into account. The information about all necessary WPs and how they can be concatenated is then represented in form of a directed graph for structured representation, see Fig. 8 for a simplified example. A node represents the state x_s of the robot after execution of a WP. The WPs themselves are represented by the edges.

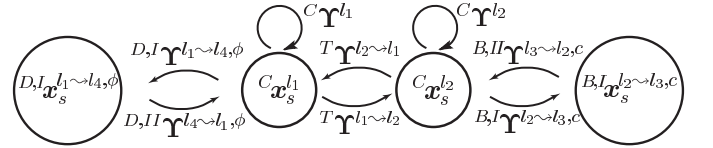


Fig. 8. Graph Representation of example WP database.

The example database represented by the graph in Fig. 8 comprises two cyclic, two transition, two barrier and two curve WPs. Starting from the state of the robot ${}^C x_s^1$ as an example, the concatenation ${}^C\Upsilon^{l_1} | {}^C\tilde{\Upsilon}^{l_1} | {}^T\Upsilon^{l_1 \sim l_2} | {}^C\tilde{\Upsilon}^{l_2} | {}^{B,I}\Upsilon^{l_2 \sim l_3, c} | {}^{B,II}\tilde{\Upsilon}^{l_3 \sim l_2, c}$ is possible, which corresponds to two steps with step length l_1 , followed by two steps with step length l_2 completed by two steps over a barrier with clearance c .

Details about the different WPs and how they are generated are discussed in the next subsections referring to the simplified example database depicted in Fig. 8. As simplification, the average speed is assumed constant for all WPs and the step times t_s are chosen appropriately in the following. Furthermore, the ratios t_1/t_s and t_2/t_s are assumed fixed.

B. Cyclic Walking Primitive

Cyclic WPs are the first WPs to be synthesized during WP database generation. A cyclic WP ${}^C\Upsilon^{l_1}$ allows continuous symmetric straight ahead walking with a constant step length $l = l_1$ by concatenation of ${}^C\Upsilon^{l_1} | {}^C\tilde{\Upsilon}^{l_1} | {}^C\Upsilon^{l_1} | \dots$. In order to obtain a cyclic WP, the boundary conditions ${}^C x_s^1 = {}^C \tilde{x}_0^1$ allowing WP concatenation and the boundary

conditions Eq. (1) and Eq. (4), where $l_I = l_{II} = l_1$, $\phi_0 = \phi_s = 0^\circ$, $w_0 = w_s = w$, are imposed on a general WP, see also [12, 17].

In addition to the desired motion, the final state of a cyclic WP ${}^C \mathbf{x}_s^{l_1} = {}^C \tilde{\mathbf{x}}_0^{l_1}$ is gained as a result, which will define the initial and final states of the WPs described in the following sections, c.f. Fig. 8.

C. Transition Walking Primitive

As a transition between two cyclic WPs ${}^C \Upsilon^{l_1}$ and ${}^C \Upsilon^{l_2}$ with different step lengths $l_1 \neq l_2$ a transition walking primitive ${}^T \Upsilon^{l_1 \rightsquigarrow l_2}$ is defined. In order to obtain a continuous state trajectory after concatenating ${}^C \tilde{\Upsilon}^{l_1} | {}^T \Upsilon^{l_1 \rightsquigarrow l_2} | {}^C \tilde{\Upsilon}^{l_2}$, initial and final states of the transition primitive have to match the corresponding states of the cyclic primitives, c.f. Fig. 8. This is ensured by the boundary conditions ${}^T \mathbf{x}_0^{l_1 \rightsquigarrow l_2} = {}^C \mathbf{x}_s^{l_1}$ and ${}^T \mathbf{x}_s^{l_1 \rightsquigarrow l_2} = {}^C \mathbf{x}_0^{l_2}$.

D. Barrier Walking Primitives

To step over a barrier, two steps and thus a concatenation of two walking primitives is necessary since the robot must place one foot over the barrier (WP I), before it can lift the trailing foot over the obstacle (WP II). This is achieved by the WP combination ${}^{B,I} \Upsilon^{l_2 \rightsquigarrow l_3, c} | {}^{B,II} \tilde{\Upsilon}^{l_3 \rightsquigarrow l_2, c}$, see Fig. 9 for an optimization result.

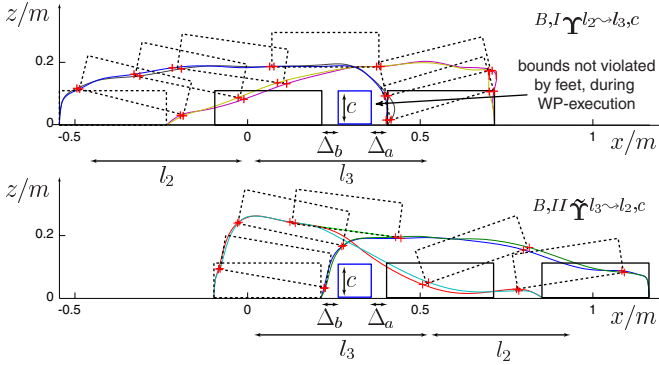


Fig. 9. Numerical results: Stepping over a barrier.

To allow WP concatenation, the initial state of the first WP must match the final state of the cyclic WP ${}^C \Upsilon^{l_2}$, c.f. Fig. 8. Accordingly, the final state of the second WP must match the initial state of ${}^C \Upsilon^{l_2}$. This is ensured by boundary conditions. The final state of the robot after execution of the first WP ${}^{B,I} \Upsilon^{l_2 \rightsquigarrow l_3, c}$, which must correspond to the initial state of the second WP ${}^{B,II} \tilde{\Upsilon}^{l_3 \rightsquigarrow l_2, c}$, is not known in advance. Thus, the two WPs cannot be computed independently. Therefore, the walking primitives are obtained by optimizing a combination of two general walking primitives together in one optimization problem comprising 6 phases. To ensure a space, which is not violated by the feet during WP execution and thus allows to step over an obstacle, inequality constraints depending on the clearance c are imposed on the direct kinematics, see Fig. 9. The parameters Δ_a and Δ_b , which define the beginning and the end of the collision free space, are assumed to be constants for simplicity.

E. Curve Walking Primitives

A change in walking direction by an angle ϕ is achieved by the combination of the two WPs ${}^{D,I} \Upsilon^{l_1 \rightsquigarrow l_4, \phi}$ and ${}^{D,II} \Upsilon^{l_4 \rightsquigarrow l_1, \phi}$. With the first WP, the swinging foot is set in the new walking direction, i.e. it

is rotated by an angle $\phi_s = \phi$ with respect to the supporting foot. At the end of the second WP, the feet reside parallel to each other and flat on the ground again (Fig. 10 and Fig. 11). As with the synthesis of barrier WPs, curve WPs result from a six phase optimal control problem. To avoid collisions between the legs for bigger angles ϕ , a larger step-width w_s at the end of the first WP is appropriate. As depicted in Fig. 11, the concatenation ${}^{D,I} \Upsilon^{l_1 \rightsquigarrow l_4, \phi} | {}^{D,II} \tilde{\Upsilon}^{l_4 \rightsquigarrow l_1, \phi}$ corresponds to a right and ${}^{D,I} \tilde{\Upsilon}^{l_1 \rightsquigarrow l_4, \phi} | {}^{D,II} \Upsilon^{l_4 \rightsquigarrow l_1, \phi}$ corresponds to a left turn.

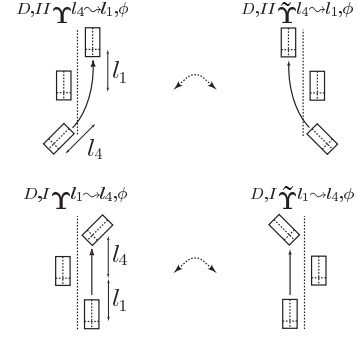


Fig. 10. Generated (left) and mapped (right) curve WPs.

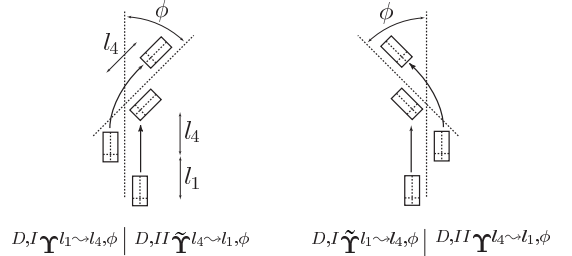


Fig. 11. Right turn and left turn after concatenation of curve WPs.

IX. SIMULATION RESULTS

As a further validation for the feasibility of walking patterns $\mathbf{q}_{ref}(t), \boldsymbol{\tau}_{ref}(t)$ gained by WP concatenation, dynamic simulations are conducted. Contrary to the rigid body contact modeling used during optimization, foot contacts are modeled by spring-damper pairs. Three spring-damper pairs are located in each of the 8 contact points \mathbf{r}_{Ri} resp. \mathbf{r}_{Li} , $i = 1 \dots 4$ situated in the corners of the two feet, see Fig. 2. In horizontal direction, linear spring damper combinations are assumed. The dampers in vertical direction are nonlinear [18]. A simple PD-control law with the precomputed computed torque term $\boldsymbol{\tau}_{ref}$ is applied for tracking control:

$$\boldsymbol{\tau} = k_p(\mathbf{q}_{ref} - \mathbf{q}) + k_d(\dot{\mathbf{q}}_{ref} - \dot{\mathbf{q}}) + \boldsymbol{\tau}_{ref} \quad (12)$$

Sensor information about the absolute pose of the walking machine in space is not used for feedback.

One simulation result is given exemplarily in Fig. 12. The path of the ZMP for the overall system as well as the projection of the center of mass to the ground (PCOM) are plotted. The average velocity of the biped is $v = 0.45 \text{ m/s}$. The robot starts from an immobile state and executes a step of 0.36m using a starting WP. It then executes a sequence of straight steps with the lengths 0.36m, 0.24m, 0.24m and 0.36m executing the WP concatenation ${}^C \tilde{\Upsilon}^{0.36} |$

$T\Upsilon^{0.36\sim 0.24} \mid C\tilde{\Upsilon}^{0.24} \mid T\Upsilon^{0.24\sim 0.36}$. This is followed by three executions of $D,I\tilde{\Upsilon}^{0.36\sim 0.36,15} \mid D,II\Upsilon^{0.36\sim 0.36,15}$ resulting each in a change of direction of $\phi = 15^\circ$. After executing the step lengths 0.44m, 0.50m, 0.36m, 0.36m half a circle is walked before the robot steps over a combination of barriers by a repeated execution of $B,I\tilde{\Upsilon}^{0.44\sim 0.44,0.16} \mid B,II\Upsilon^{0.44\sim 0.44,0.16}$ thereby lifting its feet to a clearance of $c = 0.16\text{m}$. As the reference trajectory ends, the reference for the joint angles becomes a constant value during double support and the robot swings between the front and back foot before it comes to a halt.

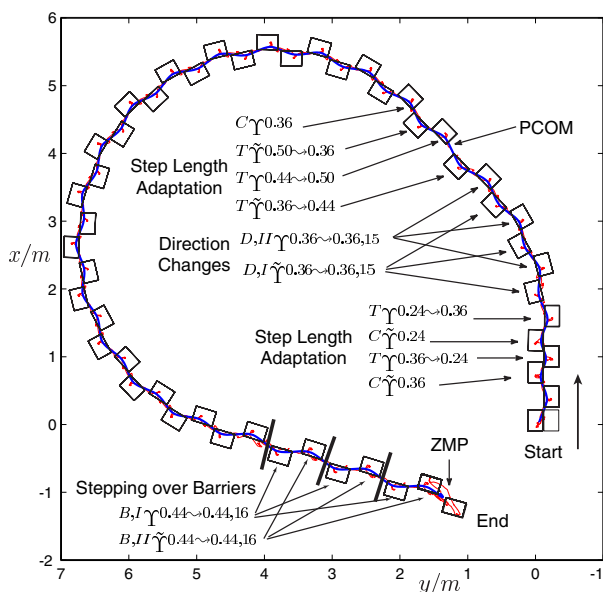


Fig. 12. Simulated walk using spring-damper contacts.

X. CONCLUSIONS AND FUTURE WORK

The contribution of this paper is a systematic method for generating databases of walking primitives for humanoid robots allowing step length adaptation, direction changes and stepping over obstacles. It is demonstrated that walking primitives can be computed efficiently by optimal control techniques using direct collocation methods. The resulting walking primitives are physically feasible and they are dynamically resp. statically stable depending on the walking speed. The approach is well suited for automatically generating databases of walking primitives, since convergence can be greatly enhanced by starting optimization runs for new walking primitives with previously gained solutions for similar problems. The information about the walking primitive database stored in the proposed graph structure together with perceptual information about the environment can be used by a step sequence planner to search for walking primitive combinations allowing a biped robot to follow a local path towards a goal position while stepping over obstacles [6].

First experiments with biped “Johnnie” [13] indicate, that the trajectories gained by the proposed performance index are only partially suitable for execution on a physical robot since joint accelerations can be unnecessarily high. However, successful walking could be achieved by regarding accelerations directly in the performance index. Our future research will therefore be directed to tailoring the trajectories to

the needs of a physical biped by an appropriate choice of the performance index and/or further restrictions of the search space.

XI. ACKNOWLEDGMENTS

This work was supported in part by the Deutsche Forschungsgemeinschaft (DFG) within the “Autonomous Walking” Priority Research Program. We would also like to express our gratitude to O. von Stryk and P. E. Gill for making their programs DIRCOL and SNOPT available for this research.

REFERENCES

- [1] G. A. Pratt, “Legged Robots at MIT: What is new since Raibert?,” *Climbing and Walking Robots: CLAWAR News*, vol. 4, pp. 4–7, February 2000.
- [2] S. Kajita, F. Kanehiro, K. Kaneko, K. Fujiwara, K. Yokoi, and H. Hirukawa, “A Realtime Pattern Generator for Biped Walking,” in *Proceedings of the IEEE International Conference on Robotics and Automation*, (Washington DC, USA), pp. 31–37, 2002.
- [3] K. Nishiwaki, T. Sugihara, S. Kagami, M. Inaba, and H. Inoue, “Online Mixture and Connection of Basic Motions for Humanoid Walking Control by Footprint Specification,” in *Proceedings of the IEEE Int. Conf. on Robotics and Automation*, (Seoul, Korea), pp. 4110–4115, 2001.
- [4] J. J. Kuffner, Jr., K. Nishiwaki, S. Kagami, M. Inaba, and H. Inoue, “Foot-step Planning Among Obstacles for Biped Robots,” in *Proceedings of the IEEE/RSJ International Conference on Intelligent Robots and Systems (IROS)*, (Maui, Hawaii, USA), pp. 500–505, 2001.
- [5] M. Yagi and V. Lumelsky, “Biped Robot Locomotion in Scenes with Unknown Obstacles,” in *Proceedings of the IEEE International Conference on Robotics and Automation*, (Detroit, Michigan), pp. 375–380, 1999.
- [6] O. Lorch, A. Albert, J. Denk, M. Gerecke, R. Cupec, J. F. Seara, W. Gerth, and G. Schmidt, “Experiments in Vision-Guided Biped Walking,” in *Proceedings of the IEEE/RSJ International Conference on Intelligent Robots and Systems (IROS)*, (Lausanne, Switzerland), pp. 2484–2490, 2002.
- [7] C. L. Shih et al., “Trajectory Synthesis and Physical Admissibility for a Biped Robot During the Single-Support Phase,” in *Proceedings of the IEEE International Conference on Robotics and Automation*, (Cincinnati, Ohio), pp. 1646–1652, 1990.
- [8] M. Hardt, J. Helton, and K. Kreutz-Delgado, “Optimal Biped Walking with a Complete Dynamical Model,” in *Proc. of the 38th IEEE Conf. on Decision and Control*, (Phoenix, AZ), pp. 2999–3004, December 1999.
- [9] P. Channon, S. Hopkins, and D. Pham, “Derivation of optimal walking motions for a bipedal walking robot,” *Robotica*, vol. 10, pp. 165–172, 1992.
- [10] C. Chevallereau and Y. Aoustin, “Optimal reference trajectories for walking and running of a biped robot,” *Robotica*, vol. 19, pp. 557–569, 2001.
- [11] M. Vukobratović, B. Borovac, D. Surla, and D. Stokić, *Biped Locomotion*, vol. 7 of *Scientific Fundamentals of Robotics*. Berlin, Germany: Springer-Verlag, 1 ed., 1990.
- [12] J. Denk and G. Schmidt, “Synthesis of a Walking Primitive Database for a Humanoid Robot using Optimal Control Techniques,” in *Proceedings of IEEE-RAS International Conference on Humanoid Robots (HUMANOIDS2001)*, (Tokyo, Japan), pp. 319–326, November 2001.
- [13] M. Gienger, K. Loeffler, and F. Pfeiffer, “Towards the Design of a Biped Jogging Robot,” in *Proceedings of the IEEE International Conference on Robotics and Automation*, (Seoul, Korea), pp. 4140–4145, 2001.
- [14] O. von Stryk, *User’s Guide for DIRCOL: A Direct Collocation Method for the Numerical Solution of Optimal Control Problems*. Lehrstuhl für Höhere Mathematik und Numerische Mathematik, Technische Universität, München, 2.1 ed., 1999.
- [15] P. E. Gill, W. Murray, and M. A. Saunders, *User’s Guide for SNOPT 5.3: A Fortran Package for Large-Scale Nonlinear Programming*. Department of Mathematics, University of California, San Diego, 2.1 ed., 1999.
- [16] T. R. Kane and D. A. Levinson, *DYNAMICS ONLINE*. OnLine Dynamics, Inc., Sunnyvale, USA, 1996.
- [17] O. Lorch, J. Denk, J. F. Seara, M. Buss, F. Freyberger, and G. Schmidt, “ViGWaM — An Emulation Environment for a Vision Guided Virtual Walking Machine,” in *Proceedings of the IEEE/RAS Int. Conf. on Humanoid Robots (Humanoids)*, (Cambridge, Massachusetts, USA), 2000.
- [18] D. W. Marhefka and D. E. Orin, “Simulation of Contact Using a Nonlinear Damping Model,” in *Proceedings of the IEEE Int. Conference on Robotics and Automation*, (Minneapolis, Minnesota), pp. 1662–1668, 1996.